# THE THERMO-HYDRODYNAMICS OF A CONCENTRIC OHMIC HEATER FOR PROCESSING DAIRY FLUIDS

**H.J. Tham[1a] , X.D. Chen[2] , B.Young[1] , B. Bansal[1*], L. Zhang[1], G. Duffy[1]**

[1] Department of Chemical & Materials Engineering, University of Auckland, New Zealand.
[a] E-mail: htha007@ec.auckland.ac.nz
[2] Department of Chemical Engineering, Monash University, Australia.

## ABSTRACT

The thermo-hydraulic performance of a 300W concentric annular ohmic heater was investigated. To minimize possible electrochemical reactions and corrosion, a higher frequency was applied and factors of field strength and frequency were studied. 2D computer simulation solving momentum, thermal and electrical energy was performed using the FlexPDE software. A good agreement between experimental and analytical analysis of static heating was obtained. There were significant differences between calculated and measured wall temperature near the entrance. The calculated outlet temperature was however in reasonable agreement with the experiment value.

## INTRODUCTION

Fouling of heat exchangers in the dairy industry has been a problem for very long time. Compared to other industries where heat exchangers may only require annual cleaning, the daily cleaning routine of the dairy industry reveals the seriousness of fouling in this industry (Changani *et al.*, 1997). Costs related to fouling include the loss of processing time, cleaning costs and effluent treatment expenses. Many factors contribute to the fouling of heat exchangers during milk heat treatment including surface temperature, flow and pH. There are also seasonal changes in the amount of fouling resulting from changes in the milk.

Ohmic heating is an alternative heating process whereby heat energy is generated within the food by its electrical conductivity. In conventional indirect heating, a heated surface is presence and heat is transferred through conduction. In static ohmic heater, it was found that electrode surface temperatures were 2 to 3°C less than the bulk temperature (de Alwis *et al.*, 1989). It was proposed that conduction from fluid dominates as the electrode material has very low resistance. This is a distinct advantage for dairy products which suffer fouling due to overheated surfaces. However, in a continuous system, effect of residence time can cause excess local heating of fluid near the wall. Therefore thermohydraulic condition of continuous ohmic heater should be optimized to avoid overheating (Ould El Moctar *et al.*, 1996).

The application of ohmic heating in dairy industry is not new. Successful commercial ohmic heating systems were developed between about 1910 to the 1930 for continuous pasteurization of milk (de Alwis and Fryer, 1990). The application however was not fully developed due to hindrances such as contamination of the electrodes from electrochemical processes, lack of accurate control and lack of effective aseptic packaging techniques.

Concerns may be raised as to the possibility of electrically- induced chemical changes in the foodstuff itself. Electrochemical reaction of food components during ohmic heating is affected by frequency and electrode material (Tzedakis *et al.*, 1999). A frequency of 50 or 60 Hz has a similar electrolytic effect as direct current (Reznick, 1996). In general, a maximum current density of 4000 A/m$^2$ is recommended to minimise corrosion, taking into account variations in the electrode and electrolytes (Stirling, 1987). Previous work in this laboratory has shown significant corrosion occurred at the electrode surfaces (Bansal et al., 2005). In the current work, a frequency above 8 kHz was applied to offset this.

## THEORY

The following 2D equations for conservation of mass, momentum, thermal energy and electrical energy describe the steady-state operation during ohmic heating:

$$\nabla.\mathbf{v} = 0 \tag{1}$$

$$\rho\left(\frac{\partial v_z}{\partial r}v_r + \frac{\partial v_z}{\partial z}v_z\right) = -\frac{\partial P}{\partial z} + \rho g + \frac{1}{r}\frac{\partial}{\partial r}\left(r\mu\frac{\partial v_z}{\partial r}\right) + \frac{\partial}{\partial z}\left(\mu\frac{\partial v_z}{\partial z}\right) \tag{2}$$

$$\rho\left(\frac{\partial v_r}{\partial r}v_r + \frac{\partial v_r}{\partial z}v_z\right) = -\frac{\partial P}{\partial r} + \rho g + \frac{1}{r}\frac{\partial}{\partial r}\left(r\mu\frac{\partial v_r}{\partial r}\right) - \left(\mu\frac{v_r}{r^2}\right) + \frac{\partial}{\partial z}\left(\mu\frac{\partial v_z}{\partial z}\right) \tag{3}$$

[*] Current address: Fonterra Co-operative Group Ltd, Private Bag 11029, Palmerston North, New Zealand.

$$\rho Cp\left(\frac{\partial T}{\partial r}v_r+\frac{\partial T}{\partial z}v_z\right)=\sigma E^2+\frac{1}{r}\frac{\partial}{\partial r}\left(rk\frac{\partial T}{\partial r}\right)+\frac{\partial}{\partial z}\left(k\frac{\partial T}{\partial z}\right) \quad (4)$$

$$\nabla(\sigma\nabla V)=0 \quad (5)$$

## MATERIALS & METHODS

### Experimental

The power set up of the experimental rig consisted of an AC power supply, an impedance-matched transformer, a signal generator and a power amplifier. The heater is of concentric annular design, with electrodes made of stainless steel (Fig. 1). The heater is 11.5 cm high, with a solid-core 5.5 cm diameter inner electrode. The outer shell, which acts as the second electrode, is 7 cm in diameter. The distance between the electrodes is 7.5 mm. This design ensures a higher electric field strength (V/cm) even at a low voltage, as the distance between electrodes is small. Three K-type thermocouples are embedded (drilled) into the inner electrode at different axial length of 2.2 cm ($T_1$), 5.7 cm ($T_2$) and 8.7 cm ($T_3$) from bottom. All thermocouples are 7 mm from the electrode surface to get temperature profiles along the axis. The fluid temperature in the annulus is not measured directly apart from the inlet and outlet stream temperature. This avoids interference with electric field, although it is possible to use Teflon coated thermocouples with proper calibration. However, since the annular gap is very small, the presence of thermocouples could impede the flow or act as another location for denatured protein deposition. The outer wall of the heater is insulated. Time, voltage, current and temperatures were recorded on a data logger at an interval of 10s.

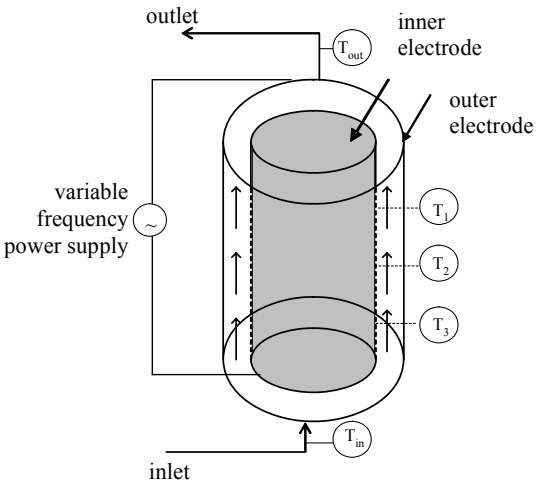


Fig. 1 Concentric annular ohmic heater

The model fluid used in this experiment was reconstituted 5% skim milk solution. Skim milk powder (NZMP, Fonterra Limited) was reconstituted using tap water. To investigate the non-fouling condition, all steady-state heating was carried out below 70°C for a period not exceeding 20 minutes. The electrical conductivity ($\sigma$) – temperature profile could be obtained by performing static ohmic heating experiments. The electrical conductivity of a sample can be calculated based on Eq. (6) and Eq. (7).

$$\sigma=\frac{d}{RA} \quad (6)$$

$$V = IR \quad (7)$$

### Numerical Simulation

Numerical simulation in two dimensions was performed using a general-purpose partial differential equation solver, FlexPDE (PDE Solutions Inc). This software uses finite element analysis to solve the equations. A student version was used in this work with limitation in grid and node. Symmetry halves the dimension of the numerical simulation.

In thick-walled tubes, the temperature of the solid wall needs to be analysed simultaneously with that of fluid. Therefore the solid-core inner electrode was included in the domain of interest to solve the temperature field. The boundary conditions used in the numerical modeling are shown in Fig. 2. This program uses a defined modeling error to control mesh generation and time step. A relative error in solution variable of 0.001 was set.

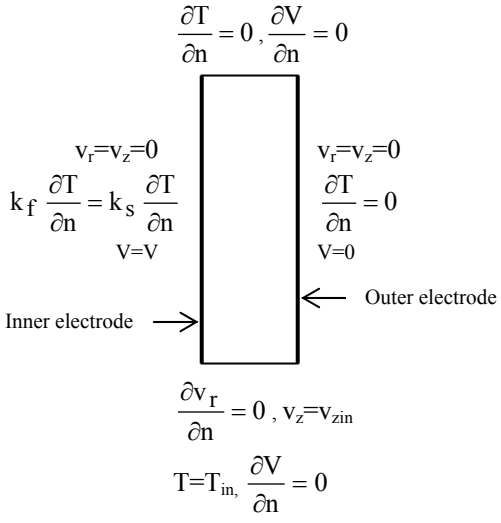


Fig. 2 Boundary conditions for the flow domain

The 'penalty' method was used to solve the Navier-Stokes equations (Backstrom, 2003). Both the flow channel and the inner electrode are included in the simulation domain. At the electrical boundary condition, a constant voltage gradient is assumed between two electrodes. Many papers report that natural convection due to density differences can cause oscillatory variation in both spatial and axial temperature profile during ohmic heating (Ould El Moctar *et al.*, 1996, El-Hajal *et al.*, 2002). In this work, due to the narrow annular gap, it is assumed that oscillatory pattern is not fully developed and hence it was ignored. The physical properties of water was used except electrical conductivity which was obtained from static experiment.

## RESULTS & DISCUSSION

### Static Heating

During static heating of the model fluid, the fluid temperature was assumed to be similar to the wall temperature. Results have shown that temperatures $T_1$, $T_2$ and $T_3$ are all overlapping indicating the temperature of liquid in the heater is uniform (Fig. 3). In all subsequent calculations for static heating, the average temperature was used.

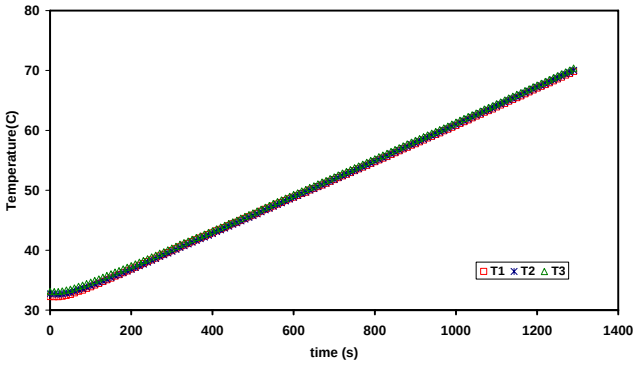


Fig. 3 Temperature variations during static heating (V=10V, 15 kHz)

It was reported that the electric field strength of volts per cm has little effect on the electrical conductivity of electrolytes (Crow, 1994). It was also shown that an applied field of <100 V/cm has negligible effects on the electrical conductivity-temperature profile of juices and liquids with inert solids. Also it has been shown that the electrical conductivity is independent of frequency below 1 GHz (Sastry, 2005). The working range of voltage used in this work was between 10 V (13.3 V/cm) and 14.5 V (19.3 V/cm), while the AC frequencies used were between 8 kHz and 15 kHz. The electrical conductivity of the model fluid at 50°C is shown in Fig. 4 and Fig. 5, it suggests that the influence of applied voltage and frequency on electrical conductivity is negligible. The values presented are the average of at least two runs. The minimum and maximum electrical conductivity for 12V at different frequency was 0.4 S/m and 0.44 S/m respectively.

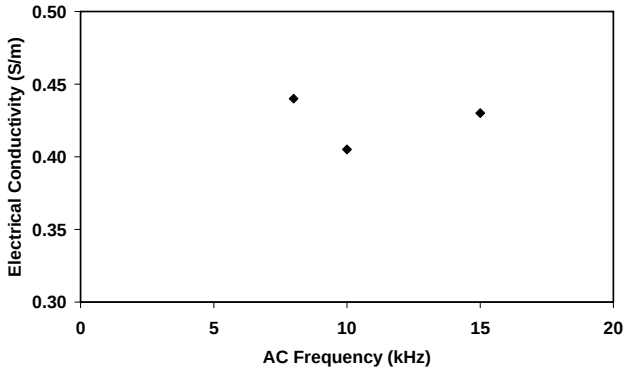


Fig. 4 Electrical conductivity of the model fluid at 50°C under different AC frequency (12 V)

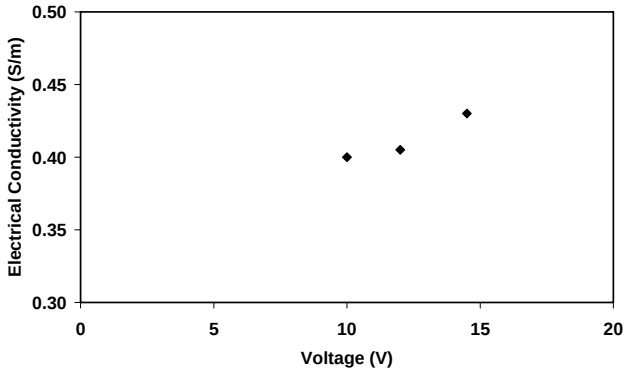


Fig. 5 Electrical conductivity of the model fluid at 50°C under different applied voltage (10 kHz)

Figure 6 shows the relationship between electrical conductivity of the model fluid and temperature under various voltages and frequencies. A linear trend line ($R^2$>0.99) plotted through the data can be described by Eq. (8). All data lie within ±5% of the linear line.

$$\sigma = 0.0057T + 0.1276 \quad (8)$$

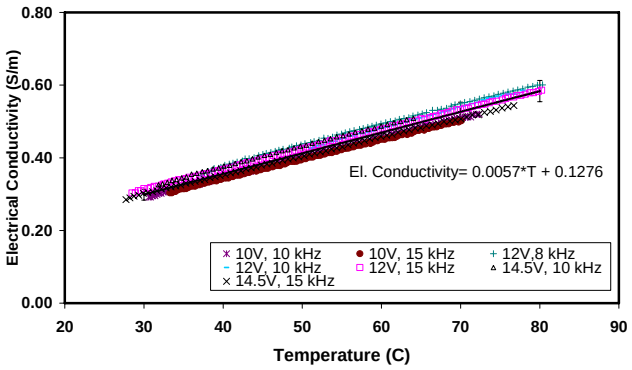


Fig. 6 Electrical conductivity - temperature relationship under various voltage and AC frequency

To analyse heat loss to the surroundings during static heating, a combined (conduction and convection) thermal resistance can be determined from Eq. (9). From experimental data, an average thermal resistance value of 4 °C/W was used in this work.

$$Rt = \frac{\overline{T} - T_a}{Q_{loss}} \tag{9}$$

Due to the design and material of construction of the heater, heat up-take by solid is taken into account and the static heat balance is:

$$(m_s Cp_s + m_f Cp_f)\frac{dT}{dt} = V^2 \overline{\sigma} \frac{A}{d} - \frac{\overline{T} - T_a}{Rt} \tag{10}$$

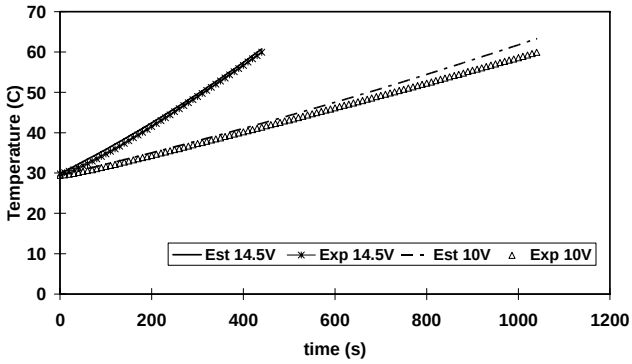


Fig. 7 Heating curves using different applied voltage

Figure 7 shows the comparison of experimental and estimated (Eq.(10)) temperature history for two different applied voltages. From the experimental results, the time required to heat the fluid from 30°C to 60°C was 440s with an applied voltage of 14.5V. It took 1040s with only 10V applied. The estimated temperature-time plot for 14.5V agrees well with the experimental heating curves. For 10V, the estimated temperature was slightly higher than the experimental values, with a maximum difference of 5%. This can be due to the increased heat loss when the experiment is run for longer.

**Continuous Heating**

Energy generated due to electrical resistance of the fluid causes a change in thermal energy of the milk between inflow and outflow. The overall steady state heat balance of the ohmic heating can be written as:

$$V.I = \dot{m} Cp_f (T_{out} - T_{in}) + Q_{loss} \tag{11}$$

The efficiency of the ohmic heater can be determined by the ratio of energy required to heat the sample (second term of Eq. (11)) to the energy supplied to the system (first term of Eq. (11)). In this work, it was assumed that all electrical energy were converted to heat. It was found from the experimental results for the steady-state operation that the efficiency is between 90% and 100%. However, for simplification, it was assumed that heat loss is negligible in the numerical simulations.

Experimental and simulation of continuous ohmic heating using applied voltage of 12V, inlet temperature of 52.6°C and Reynolds number of 180 was performed. The governing equations described earlier in the theory section were solved simultaneously to obtain the temperature profile during continuous ohmic heating. From Fig. 8, the centerline bulk temperature variation along the axial length was almost linear. The outer wall temperature is almost parallel to the bulk temperature. On the other hand, as a result of heat distributed downwards due to axial solid conduction in the thick wall, the inner wall temperature is much lower then the outer wall temperature towards the exit.

Figure 9 presents the results for the scenario of a thin-walled hollow annular tube with the same inner and outer radius as the solid-core annular heater. In this case both inner and outer wall were assumed to be adiabatic. The temperature distribution of the inner and outer wall are obviously different than that of Figure 8. There is a small difference in temperature between the walls. This may be an effect of curvature. Simulation for a narrow gap annulus with large radius may show this.

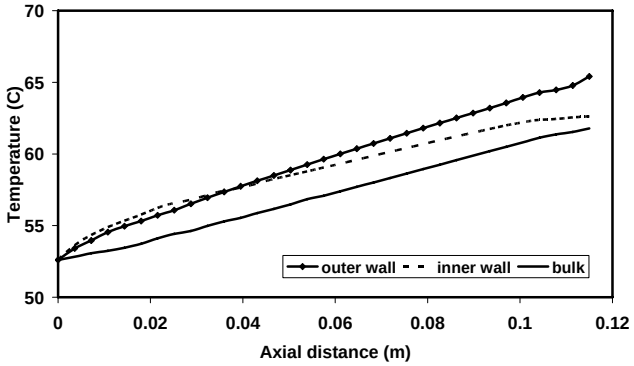


Fig. 8 Simulated temperature along axial length

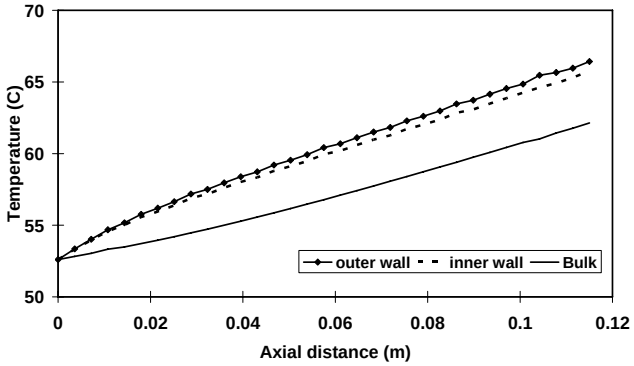


Fig. 9 Simulated temperature along axial length for thin-wall tube

Figure 10 shows the numerical and measured temperatures at different locations. The three measured values are almost constant over the length, while the numerical results show an almost linear trend. The possible reason for the deviation could be entrance effects, and non-uniform flow distribution near the entrance. Wall conduction can also affect heat transfer characteristics especially near the entrance and exit (Sakakibara *et al.*, 1987). For the bulk outlet temperatures, the simulation result was 61.8°C, while the experimental work gave a value of 59.5°C. Taking into account instrumental error, truncation and rounding error in the numerical simulation, the discrepancy is considered within practical range.

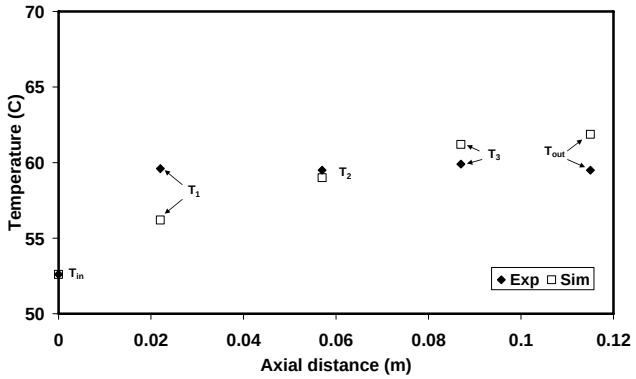


Fig.10 Measured temperature and numerically determined temperature along the vertical axis (12V, $T_{in}$=52.6°C, Re=180)

## CONCLUSIONS

The experimental and numerical analyses of both static and continuous ohmic heating of skim milk under non fouling conditions have been presented. The electrical conductivity-temperature relationship for a 5% reconstituted skim milk was determined. The influence of applied voltage and AC frequency on conductivity-temperature relationship is negligible over the range of conditions used here. There is good agreement between the experimental and analytical analyses for the static heating investigations. Numerical analysis for steady-state laminar flow shows that conduction of the solid-cored wall plays an important role in the redistribution of wall temperature. Significant differences between the measured and calculated values from numerical simulation of wall temperature near the entrance were obtained. However, the outlet temperatures calculated from numerical simulation were in close agreement with the measured values. The next step is to investigate how the thermal behaviour of this concentric annular ohmic heater affects fouling during laminar flow at steady-state operation.

## ACKNOWLEDGEMENT

This study is financially supported by Auckland Uniservices and Education New Zealand.

## NOMENCLATURE

| | |
|---|---|
| A | electrode area, $m^2$ |
| $C_P$ | specific heat, J/kg K |
| d | distance between electrodes, m |
| E | electric field strength, V/m |

| | |
|---|---|
| g | gravity acceleration, $m/s^2$ |
| I | measured current, A |
| k | thermal conductivity, W/m K |
| m | mass, kg |
| $\dot{m}$ | mass flow rate, kg/s |
| n | normal direction |
| P | pressure, Pa |
| $Q_{loss}$ | Energy loss, W |
| r | radial coordinate, m |
| R | resistance, ohm |
| Rt | thermal resistance, °C/W |
| t | time, s |
| T | temperature, $^oC$ |
| $\overline{T}$ | average temperature, $^oC$ |
| **v** | velocity vector |
| v | velocity, m/s |
| V | applied voltage, V |
| z | axial coordinate, m |

**Greek**

| | |
|---|---|
| μ | viscosity, kg/m s |
| ρ | density, $kg/m^3$ |
| σ | electrical conductivity, S/m |

**Subscripts**

| | |
|---|---|
| 1,2,3 | Axial location of thermocouple |
| a | ambient |
| b | bulk |
| f | fluid |
| in | inlet |
| out | outlet |
| r | radial direction |
| s | solid |
| z | axial direction |

## REFERENCES


Backstrom, G., 2003, *Fluid dynamics by finite element analysis,* GB Publishing.

Bansal, B., Chan, X. D. and Lin, X. Q.,2005, Skim milk fouling during ohmic heating, *Proc. 6th International Conference on Fouling and Cleaning - Challenges and Opportunities*, Germany, pp. 133-140

Changani, S. D., Belmar-Beiny, M. T. and Fryer, P. J., 1997, Engineering and chemical factors associated with fouling and cleaning in milk processing, *Experimental Thermal and Fluid Science,* Vol.14, pp.392-406.

Crow, D. R., 1994, *Principles and applications of electrochemistry,* Blackie Academic and Professional, Glasgow, UK.

de Alwis, A. A. P. and Fryer, P. J., 1990, The use of direct resistance heating in the food industry, *Journal of Food Engineering,* Vol.11, pp.3-27.

de Alwis, A. A. P., Halden, K. and Fryer, P. J., 1989, Shape and conductivity effects in the ohmic heating of foods, *Chem Eng Res Des,* Vol.67, pp.159-167.

El-Hajal, J., Moctar, A. O. E. and Peerhossaini, H., 2002, Velocity and temperature fields in a plane poiseuille flow with volume heating: Measurements under electric field, *Experimental Heat Transfer,* Vol.15, pp.137-159.

Ould El Moctar, A., Peerhossaini, H. and Bardon, J. P., 1996, Numerical and experimental investigation of direct electric conduction in a channel flow, *International Journal of Heat and Mass Transfer*, Vol.39, pp.975-993.

PDE Solutions Inc, 2005, www.pdesolutions.com.

Reznick, D., 1996, Ohmic heating of fluid foods, *Food Technology,* Vol.50, pp.250-251.

Sakakibara, M., Mori, S. and Tanimoto, A., 1987, Conjugate heat transfer with laminar flow in an annulus, *Can. J. Chem. Eng.,* Vol.65, pp.541-549.

Sastry, S. K., 2005, Electrical conductivity of foods, in *Engineering properties of foods*, eds.Rao, M. A., Rizvi, S. S. H. and Datta, A. K., Taylor & Francis, Boca Raton, pp. 461-497.

Stirling, R., 1987, Ohmic heating-a new process for the food industry, *Power Engineering J.,* Vol.6, pp.365-371.

Tzedakis, T., Basseguy, R. and Comtat, M., 1999, Voltammetric and coulometric techniques to estimate the electrochemical reaction rate during ohmic sterilization, *Journal of Applied Electrochemistry,* Vol.29, pp.819-826.